Pressure and Denaturants in the Unfolding of Triosephosphate Isomerase: The Monomeric Intermediates of the Enzymes from *Saccharomyces cerevisiae* and *Entamoeba histolytica*†

Adrián R. Vázquez-Pérez and D. Alejandro Fernández-Velasco*

Laboratorio de Fisicoquímica e Ingeniería de Proteínas, Departamento de Bioquímica, Facultad de Medicina, Universidad Nacional Autónoma de México, Apartado Postal 70-159, México D.F., 04510 Mexico

Received September 9, 2006; Revised Manuscript Received May 16, 2007

ABSTRACT: Triosephosphate isomerase (TIM) is a dimeric enzyme formed by two identical $(\beta/\alpha)_8$ barrels. In this work, we compare the unfolding and refolding of the TIMs from *Entamoeba histolytica* (EhTIM) and baker's yeast (yTIM). A monomeric intermediate was detected in the GdnHCl-induced unfolding of EhTIM. The thermodynamic, spectroscopic, catalytic, and hydrodynamic properties of this intermediate were found to be very similar to those previously described for a monomeric intermediate of yTIM observed in GdnHCl. Monomer unfolding was reversible for both TIMs; however, the dissociation step was reversible in yTIM and irreversible in EhTIM. Monomer unfolding induced by high pressure in the presence of GdnHCl was a reversible process. ΔG_{Unf}, ΔV_{Unf}, and $P_{1/2}$ were obtained for the 0.7−1.2 M GdnHCl range. The linear extrapolation of these thermodynamic parameters to the absence of denaturant showed the same values for both intermediates. The ΔV_{UnfH_2O} values calculated for EhTIM and yTIM monomeric intermediates are the same within experimental error (−57 ± 10 and −76 ± 14 mL/mol, respectively). These $\Delta V_{Unf\ H2O}$ values are smaller than those reported for the unfolding of monomeric proteins of similar size, suggesting that TIM intermediates are only partially hydrated. $|\Delta V_{Unf}|$ increased with denaturant concentration; this behavior is probably related to structural changes in the unfolded state induced by GdnHCl and pressure. From the thermodynamic parameters that were obtained, it is predicted that in the absence of denaturants, pressure would induce monomer unfolding ($P_{1/2} \sim 140$ MPa) prior to dimer dissociation ($P_{1/2} \sim 580$ MPa). Therefore, dimerization prevents the pressure unfolding of the monomer.

A central theme regarding oligomeric proteins is the role of subunit association in the function, stability, and structure of the complex (*1*, *2*). The thermodynamic description of the folding mechanism of proteins has been investigated using temperature, chemical denaturants, and pressure as perturbants (*2*−*10*). Pressure has been shown to be a useful method for characterizing the differences in stability and volume that accompany protein dissociation and unfolding reactions (*11*−*16*). The effect of pressure seems to be strongly dependent on the particular properties of the protein under study. Upon pressurization, proteins might unfold (*13*, *17*−*21*) or remain unaffected (*22*, *23*). In the study of noncovalent protein complexes formed by the association of complementary fragments (*23*), pressure has been shown as an alternative to characterize unfolding in the absence of chemical denaturants. Folding intermediates may be stabilized or destabilized when pressure is applied (*24*−*27*); pressure promotes refolding (*28*−*30*) but in other cases leads to aggregation (*31*). All these apparently contradictory or unrelated effects of pressure are governed only by the volume decrease of the protein−solvent system, as predicted by Le Chatelier's principle. Chemical denaturants have been used in combination with pressure to study the volume changes of folding intermediates (*27*, *32*−*34*), to characterize stable proteins (*23*, *32*), and to study the dissociation of oligomeric proteins (*22*, *35*). In this work, we used high pressure and guanidinium hydrochloride (GdnHCl) to characterize the unfolding−refolding mechanism of the monomeric intermediates observed in the refolding of the dimeric enzyme triosephosphate isomerase (TIM). TIM is the prototype of $(\beta/\alpha)_8$ barrels. In mesophiles, this glycolytic enzyme is built by two identical subunits of 26−28 kDa. The structure and catalytic properties of TIMs have been explored thoroughly (*36*−*42*). Wild-type TIMs are active only in their native dimeric form. Monomeric folding intermediates characterized in kinetic (*43*−*46*) and equilibrium (*47*−*49*) studies as well as monomers obtained through chemical derivatization are inactive (*50*). Moreover, genetically engineered monomeric forms of TIM present, at best, a catalytic activity 100 times lower than that of wild-type TIM (*51*−*53*).

The denaturant-induced unfolding of human and rabbit TIM (hTIM and rTIM, respectively) (*54*−*56*) has been described as a two-state process under equilibrium conditions. Nevertheless, monomeric and dimeric intermediates, including complex reversible and irreversible schemes, have also

† This work was partially supported by grants from CONACYT (43592-Q and 41328-Q).

* To whom correspondence should be addressed. E-mail: fdaniel@servidor.unam.mx. Telephone: 52 55 56 23 22 59. Fax: 52 55 56 16 24 19.

10.1021/bi061879j CCC: $37.00
Published on Web 06/27/2007

been reported (*47*, *49*, *57*−*60*). In addition, deterministic behavior has been proposed for the dissociation of rTIM induced by pressure (*61*) or GdnHCl (*55*, *62*). Although the folding behavior of TIM seems to be diverse, it is clear that association accounts for most of the stability of the enzyme (*48*, *49*, *54*, *55*). In the case of TIM from the yeast *Saccharomyces cerevisiae* (yTIM), unfolding and refolding studies using GdnHCl (*48*, *63*), urea (*48*), or temperature (*64*, *65*) lead to the following folding mechanism: $N \leftrightarrows 2M \leftrightarrows 2U$. The bimolecular step was assigned on the basis of the displacement of reactivation curves to lower GdnHCl concentration as the yTIM concentration was decreased. Kinetic studies were compatible with the aforementioned mechanism (*64*). The monomeric intermediate (M) of yTIM characterized in GdnHCl is inactive and expanded and retains considerable secondary structure, while its aromatic residues seem to be partially buried (*48*). Even though TIM structure is quite conserved, the top and bottom loops forming the barrel present interesting differences among species. For example, when compared with yTIM, the TIM from *Entamoeba hystolytica* (EhTIM) presents 14 insertions mainly located in the loops connecting α helices with β strands (*50*). The unfolding mechanism of EhTIM has not been characterized. In this work, we characterized a monomeric intermediate found in the GdnHCl-induced unfolding and refolding of EhTIM. This intermediate was then compared with the yTIM intermediate previously found at very similar denaturant concentrations. Finally, both monomers were further characterized by means of high-pressure perturbation in the presence of GdnHCl.

MATERIALS AND METHODS

Glycerol-3-phosphate dehydrogenase (GDPH) and guanidinium hydrochloride (GdnHCl) were purchased from Boehringer-Mannheim. All other reagents were purchased from Sigma. Production, expression, and purification of recombinant yTIM (*66*) and EhTIM (*67*) were performed as previously described. Unless otherwise stated, unfolding and refolding experiments were carried out at 25 °C in solutions containing variable amounts of GdnHCl. The buffer used in this work consists of 100 mM triethanolamine, 10 mM EDTA, and 1 mM dithiothreitol (DTT), pH 7.4 (TED buffer).

GdnHCl-Induced Unfolding and Refolding. TIM solutions were incubated in 4.0 M GdnHCl for 1 h; this led to complete unfolding of TIM as indicated by the complete inactivation of the enzyme, a far-UV CD spectrum characteristic of unfolded proteins, a decrease in the quantum yield, and a red shift of the fluorescence spectrum. After this step, refolding was induced by dilution of the unfolded protein to lower GdnHCl concentrations and a final TIM concentration of 110 μg/mL. To achieve equilibration during refolding conditions, these samples were incubated for 24 h. The conformational properties of TIM were then followed at atmospheric or high pressure as described in what follows.

Catalytic activity was determined with a coupled enzyme assay. Reaction cells (1 mL) were prepared in TED containing 2.6 mM D-glyceraldehyde 3-phosphate, 10 μg of α-glycerolphosphate dehydrogenase, and 0.2 mM NADH. The reaction was started by the addition of 2 ng of EhTIM. Reaction rates were determined from the decrease in absorbance at 340 nm as a function of time in a Beckman DU7500 spectrophotometer with a multicell device kept at 25 ± 0.1 °C. The dilution protocol previously reported (*47*, *48*) was used to determine the catalytic activity of samples incubated in GdnHCl.

Size-exclusion chromatography experiments were performed on a Superdex 75 HR 10/30 column coupled to a Pharmacia (Uppsala, Sweden) FPLC system. Protein elution was monitored with an integrated absorbance detector, using a wavelength of 280 nm. The incubated enzymes were loaded onto the filtration column, equilibrated with TED solutions containing the appropriate amount of GdnHCl. Samples were eluted at a flow rate of 0.4 mL/min. Stokes radii (R_s) were calculated from elution volumes and a calibration curve.

Circular dichroism experiments (200 μg/mL EhTIM) were carried out in a JASCO J-715 spectropolarimeter, thermostated at 25 °C with a Peltier device. Ellipticity was followed at 222 nm using a cell with a path length of 0.1 cm. The values reported were the average of 10 min scans recorded every 20 s. Reference samples without protein were subtracted in all measurements.

All fluorescence measurements were taken on an ISS (Champaign, IL) PC1 spectrofluorimeter. The temperature of the cells was maintained at 25 ± 0.1 °C. Fluorescence measurements were carried out at an excitation wavelength of 280 nm (4 nm bandwidth), and emission was monitored from 300 to 400 nm (8 nm bandwidth). The fluorescence spectral center of mass (SCM) was calculated from intensity data (I) obtained at different wavelengths (λ) using the relationship $SCM = (\sum \lambda I_\lambda)/(\sum I_\lambda)$ (*68*). Tryptophan anisotropy measurements (110 μg/mL) were obtained using 295 nm as the excitation wavelength and 340 nm as the emission wavelength. G factors were calculated for each sample and were consistent throughout all the measurements (G factor = 2.61 ± 0.02). Anisotropy (r) is defined as $(I_{||} - I_\perp)/(I_{||} + 2I_\perp)$ (*68*).

Acrylamide Quenching of Tryptophans. To calculate the Stern−Volmer constant (K_{sv}), fluorescence emission spectra (λ_{ex} = 295 nm; λ_{em} = 305−405 nm) of TIM samples (110 μg/mL) were obtained; thereafter, small volumes of a concentrated solution of acrylamide (6.67 M) were added. The final volume of added acrylamide was less than 10% of the final solution volume. Fluorescence intensities were corrected for dilution. Fluorescence intensities in the absence (F_0) or presence (F) of a given quencher concentration ([Q]) were obtained at the wavelength of maximum emission observed for each TIM/GdnHCl solution. Acrylamide concentrations ranged from 0 to 150 mM. All samples exhibited linear behavior in this range of quencher concentrations. Experimental points were fitted to the equation $F_0/F = 1 + K_{sv}[Q]$ (*68*).

A high-pressure cell system (ISS) coupled to an automated pressure pump (APP) was used to increase pressure in TIM samples. An automatized protocol was used to obtain fluorescence spectra (λ_{ex} = 280 nm; λ_{em} = 300−400 nm) after pressure jumps of 17 MPa up to 172 MPa and then every 34 MPa up to 345 MPa. The same pressure-jump scheme was applied for depressurization measurements. Fluorescence spectra obtained at high pressures were recorded at different times after each pressure jump. All the pressure data presented were obtained after incubation for 30 min, since no further change in the spectral properties was observed after incubation for 60 or 90 min.

Data Fitting. The pressure-induced unfolding of the monomeric intermediate was analyzed using a two-state model.

$$\mathrm{M} \leftrightarrow \mathrm{U} \quad (1)$$

where M is the monomeric intermediate and U the unfolded monomer. The change in Gibbs energy for monomer unfolding at a given pressure (ΔG_P) was expressed as (*32*, *33*)

$$\Delta G_P = -RT \ln K_{eq} = -RT \ln(X_P - X_M)/(X_U - X_P) \quad (2)$$

where X_P is the spectral center of mass at a given pressure and X_M is the spectral center of mass of the monomeric intermediate. It is known that pressure has an intrinsic red shift effect on the fluorescence spectra of tryptophan residues (*69*). Therefore, in eq 2, it was assumed that the spectral center of mass of the unfolded monomer (X_U) changes linearly with pressure (P) according to the relationship $X_U = X_{U(P=0)} + bP$, where $X_{U(P=0)}$ is X_U at atmospheric pressure and b is $\delta(X_U)/\delta P$.

A constant standard volume change (ΔV_{Unf}) was used; i.e., no change in compressibility between the monomeric intermediate and unfolded monomers was assumed. Therefore, according to Le Chatelier's principle, ΔG_P changes with pressure as follows (*26*, *61*):

$$\Delta G_P = \Delta G_{P=0} + P\Delta V_{Unf} \quad (3)$$

where $\Delta G_{P=0}$ is the change in free energy at atmospheric pressure. Equations 2 and 3 were rearranged as

$$X_P = \{X_M + [X_{U(P=0)} + bP]e^{-(\Delta G_{P=0} + P\Delta V_{Unf})/RT}\}/[1 + e^{-(\Delta G_{P=0} + P\Delta V_{Unf})/RT}] \quad (4)$$

X_P values were calculated from emission spectra obtained after a 30 min equilibration at a given pressure. The parameters $\Delta G_{P=0}$, ΔV_{Unf}, b, X_M, and $X_{U(P=0)}$ were fitted to SCM versus pressure data using eq 4.

The $\Delta G_{P=0}$ and ΔV_{Unf} values thus obtained were used to calculate the pressure of half-transition ($P_{1/2}$) according to eq 5.

$$P_{1/2} = -\Delta G_{P=0}/\Delta V_{Unf} \quad (5)$$

For the analysis of the GdnHCl-induced unfolding of TIM at atmospheric pressure (*6*), ΔG_{Unf} values for a two-state transition were calculated from normalized values using the following equation:

$$\alpha = 1/[1 + e^{-(\Delta G_{H2O} + m^*[\mathrm{GdnHCl}])/RT}] \quad (6)$$

where $\alpha = [y(x) - y(x')]/[y(x=0) - y(x')]$, x' is the denaturant concentration for complete unfolding of the monomer, and y is SCM, K_{sv}, molar ellipticity, or r. Equation 6 assumes a linear dependence of ΔG_{Unf} with GdnHCl concentration (*6*).

Thermodynamic parameters (ΔG_{Unf}, ΔV_{Unf}, or $P_{1/2}$) obtained from pressure experiments in the 0.7−1.2 M GdnHCl range were also assumed to vary linearly with denaturant concentration

$$J = J_{H_2O} + m_J[\mathrm{GdnHCl}] \quad (7)$$

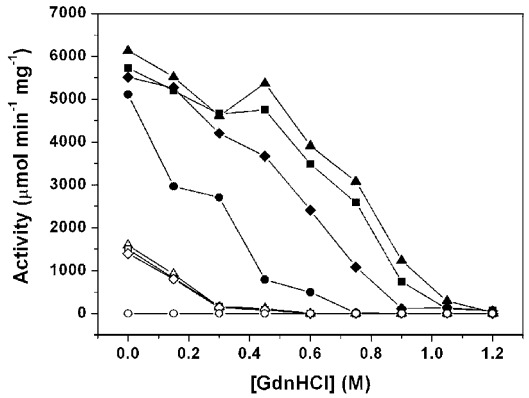

FIGURE 1: Unfolding and refolding of EhTIM followed by catalytic activity. EhTIM samples (1 μg/mL) were incubated for 24 (▲ and △), 48 (■ and □) 144 (◆ and ◇) or 288 h (● and ○) in unfolding or refolding experiments (filled and empty symbols, respectively). Catalytic activity was determined as described in Materials and Methods.

where m_J is $\delta(J)/\delta([\mathrm{GdnHCl}])$ and $J = \Delta G_{Unf}$, ΔV_{Unf}, or $P_{1/2}$. ΔV_{H_2O} was also calculated as the mean of ΔV_{Unf} values, i.e., assuming ΔV is independent of denaturant concentration.

RESULTS AND DISCUSSION

Unfolding and Refolding of EhTIM in GdnHCl. Changes in the functional properties of EhTIM induced by GdnHCl were studied in unfolding and refolding experiments (Figure 1). Hysteresis was observed between unfolding and refolding experiments. The activity of refolding samples increases with time (data not shown). The maximum activity in these samples was obtained after refolding for 24 h and remained constant for up to 144 h, and longer incubation times resulted in complete inactivation of the enzyme (empty symbols in Figure 1). On the other hand, in unfolding samples (filled symbols in Figure 1), nearly constant values were obtained for unfolding times of 24 and 48 h. However, activity decreased at longer incubation times, where visible aggregation of the protein was observed. This aggregation may explain the severe decay of catalytic activity observed in unfolding and refolding conditions after long incubation times. The maximum degree of reversibility, observed for EhTIM after refolding in 50 mM GdnHCl for 24 h, was 26% of the original catalytic activity (Figure 1).

EhTIM samples were then followed by fluorescence SCM measurements over a broad range of GdnHCl concentrations. Refolding samples reached constant values within 1 h. In contrast, unfolding samples required nearly 24 h to achieve steady values (data not shown). After incubation for 24 or 48 h, SCM values were coincident for unfolding and refolding samples (Figure 2). SCM values were nativelike from 0 to 0.75 M GdnHCl, indicating that SCM is insensitive to the transition detected by catalytic activity, and showed a single transition from 0.75 to 2 M GdnHCl (Figure 2). No further changes in SCM or in other spectroscopic techniques were detected at higher concentrations of denaturant (see below), indicating that EhTIM is completely unfolded in 2.0 M GdnHCl. The coincidence of SCM values between unfolding and refolding EhTIM samples throughout the 0−2 M GdnHCl range suggests that this spectral property follows a reversible process that is at equilibrium under the conditions shown in Figure 2. The midpoint of the transition

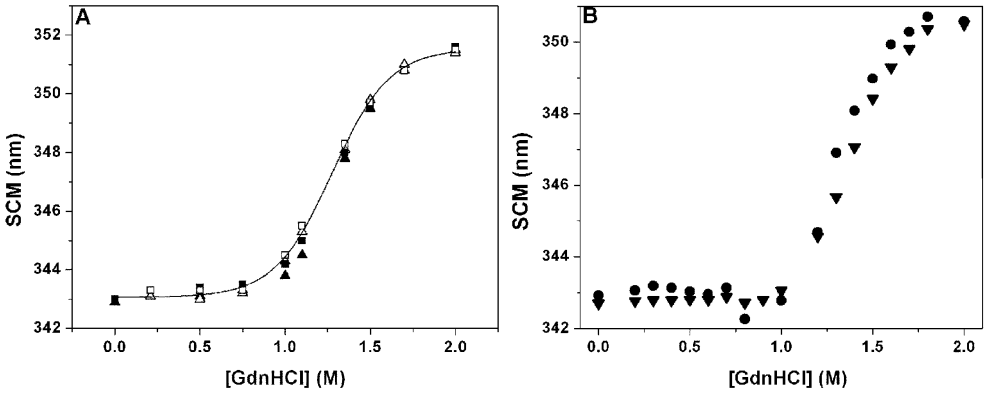

FIGURE 2: Unfolding and refolding of EhTIM followed by fluorescence SCM. (A) EhTIM samples (110 μg/mL) were incubated for 24 (▲ and △) or 48 h (■ and □) in unfolding or refolding experiments (filled and empty symbols, respectively). Fluorescence emission spectra were then obtained. (B) EhTIM samples [50 (▼) or 430 μg/mL (●)] were incubated for 24 h in unfolding experiments. Fluorescence emission spectra were then recorded.

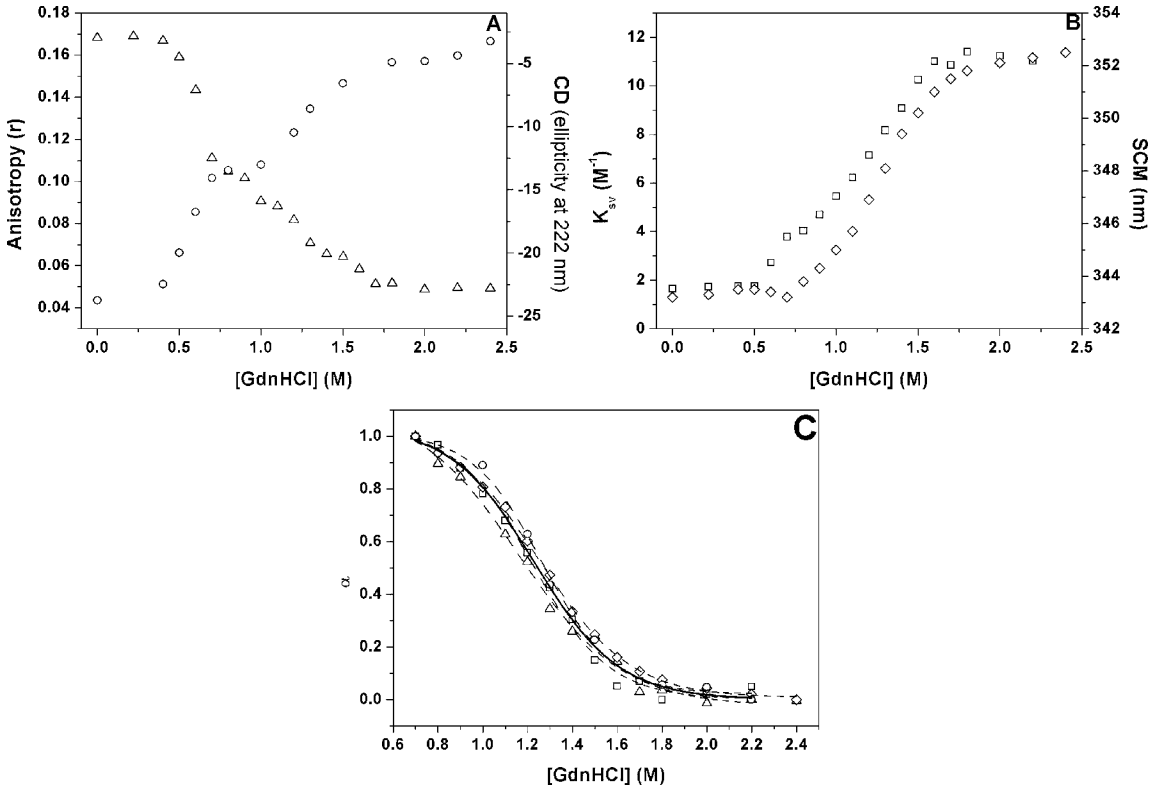

FIGURE 3: Refolding of EhTIM followed by several spectroscopic methods. EhTIM samples were incubated for 24 h under refolding conditions. Afterward, the following measurements were taken: circular dichroism at 222 nm (○, A), fluorescence anisotropy (△, A), spectral center of mass (◇, B), and Stern−Volmer constant for acrylamide−tryptophan quenching (□, B) (see Materials and Methods). Data were normalized in panel C as follows: $\alpha = [y(x) - y(x')]/[y(x=0) - y(x')]$, where x' is the denaturant concentration for complete unfolding of the monomer. Dashed lines in panel C are fits of each data set to a two-state model (eq 6). The solid line is a global fit of all data. Fitting parameters are listed in Table 2.

detected by SCM was insensitive to an 8.6-fold increase in protein concentration, suggesting that this transition is unimolecular (Figure 2B).

Taken together, Figures 1 and 2 suggest the presence of an intermediate. The transition between the native dimer and the intermediate (0−0.7 M GdnHCl) was not detected by SCM and seems irreversible regarding catalytic activity. At higher denaturant concentrations (0.7−2.0 M GdnHCl), SCM changes detected the unimolecular and reversible transition between the intermediate and the unfolded protein. The time courses of fluorescence anisotropy and SCM changes indicated that equilibrium values are reached faster in refolding than in unfolding experiments (data not shown); therefore, experiments were carried out in the refolding direction after a 24 h incubation period. Figure 3 shows such a refolding profile followed by several spectroscopic techniques.

Two transitions were observed by most techniques, confirming the presence of a folding intermediate. The first transition, clearly detected by catalytic activity (Figure 1), anisotropy, circular dichroism, and acrylamide quenching (Figure 3A,B), was observed from 0 to 0.7 M GdnHCl. The second transition (from 0.7 to 2.4 M GdnHCl) was observed by all the spectroscopic techniques (Figure 3A,B). The values of SCM (352.5 nm), anisotropy ($r = 0.049$), K_{sv} (10.74 M^{-1}),

Table 1: Comparison of EhTIM and yTIM Monomers in 0.7 M GdnHCl

	EhTIM		yTIM	
	native	0.7 M GdnHCl	native	0.7 M GdnHCl
k_{cat} (s^{-1})	1.45×10^7	inactive	1.58×10^7 [a]	inactive[a]
SCM (nm)	343.2	343.2	332.0	340.5[a]
CD at 222 nm (% of native signal)	100	50	100[a]	52[a]
fluorescence anisotropy (r)	0.169	0.111	0.112	0.109
Stern−Volmer constant (M^{-1})	1.65	3.79	3.06	3.70
Stokes radius (Å)	31.2	31.2	30.0[a]	30.0[a]

[a] Data from ref *48*.

and circular dichroism observed in 2.4 M GdnHCl are characteristic of unfolded proteins (*68*, *70*−*72*).

The intermediate exhibits 50% of the total change in the CD signal (Figure 3A) and ~25% of the total change in the Stern−Volmer constant (Figure 3B), which reflects a considerable loss of secondary structure and some gain of accessibility of acrylamide to tryptophan residues, strongly suggesting an expansion of the enzyme. To gain further insight into the association state of the intermediate, the Stokes radii of EhTIM in the presence of 0 and 1.0 M GdnHCl were determined. A single peak with a similar elution volume was detected under both conditions (data not shown); therefore, the R_s values of the intermediate and the native dimer are similar [31.2 Å (Table 1)]. These R_s values are incompatible with the intermediate being an expanded dimer and suggest the presence of an expanded monomer. The unusually high anisotropy of EhTIM in the absence of denaturant [$r = 0.169$ (Figure 3A)] indicates the existence of a high-quantum yield tryptophan residue with a long lifetime in the native enzyme. Half of the anisotropy change was observed through the first transition [$r = 0.110$ in 0.7 M GdnHCl (Table 1)], suggesting dimer dissociation and/or a considerable rearrangement of the environment surrounding tryptophan residues. Such a change in r is predicted for dimer dissociation according to Perrin's equation (assuming no change in the lifetime of the highest-quantum yield fluorophore) (*68*). In addition, this intermediate is inactive as reported for other monomeric folding intermediates (*43*, *44*, *47*, *48*), monomers obtained by chemical derivatization (*50*), and monomeric mutants of TIM (*51*, *52*). All this evidence led us to propose that the intermediate observed in EhTIM refolding is an expanded monomer. The unimolecular nature of the second transition was further confirmed by the pressure experiments presented below. Hence, the first transition corresponds to the irreversible dissociation of the native dimer ($N \rightarrow 2M$), while the second reversible transition should report on the unfolding and refolding of the monomeric intermediate ($2M \leftrightarrows 2U$). Consequently, we propose the following folding mechanism for EhTIM in GdnHCl: $N \rightarrow 2M \leftrightarrows 2D$. Thermodynamic parameters were calculated only for the second transition, fitting data obtained from 0.7 to 2.4 M GdnHCl to a two-state model (Table 2). Figure 3C shows the normalized data; a global fit including all techniques gives the following: $\Delta G_{Unf} = 16.2 \pm 1.1$ kJ/mol and $m_G = -13.2 \pm 0.85$ kJ mol^{-1} M^{-1}.

Comparison of the Folding Mechanisms of EhTIM and yTIM. The GdnHCl-induced unfolding and refolding of both yTIM and EhTIM can be adequately described by a three-state model with a monomeric intermediate. In yTIM, the first step is reversible (*48*), whereas in EhTIM, this transition is irreversible (Figure 1). The second transition is reversible for both enzymes (Figure 2 and ref *48*). To make a comprehensive comparison of both intermediates, Table 1 presents EhTIM data, anisotropy, and tryptophan quenching experiments conducted for yTIM in this work as well as previous results obtained for yTIM (*48*). yTIM has three tryptophan residues per monomer, whereas EhTIM has five; this accounts for the different SCM, anisotropy, and the Stern−Volmer constants of native EhTIM and yTIM. Considering these facts, a thorough molecular interpretation of fluorescence data is not feasible. Nevertheless, the properties of both intermediates are strikingly similar (Table 1). Both of them are inactive, and according to CD spectroscopy, they show a considerable loss of secondary structure. In agreement, size exclusion chromatography experiments indicate that both monomers present dimerlike R_s values; i.e., they are expanded. With regard to fluorescence properties in both intermediates, tryptophan residues exhibit partial accessibility to acrylamide quenching. SCM values suggest that aromatic residues have, on average, a comparable exposure to solvent molecules. With concern for anisotropy, r values for both monomers are quite close, perhaps indicating a similar correlation time. To further explore the thermodynamic properties of these monomeric intermediates, pressure unfolding experiments were performed.

Table 2: Thermodynamic Properties Obtained from Refolding Data for EhTIM[a]

	ΔG_{Unf} (kJ/mol)	m_G (kJ mol^{-1} M^{-1})	$C_{1/2}$ (M)
SCM	15.5 ± 1.6	-12.3 ± 1.2	1.25
anisotropy	12.7 ± 1.8	-10.9 ± 1.3	1.17
CD	19.9 ± 2.5	-15.7 ± 1.9	1.26
acrylamide quenching	17.7 ± 1.8	-14.5 ± 1.4	1.22
global fit	16.2 ± 1.1	-13.2 ± 0.9	1.23

[a] Fitting parameters were obtained from normalized data using the 0.7−2.4 M GdnHCl range (Figure 3C) and eq 6.

Pressure Unfolding and Refolding of EhTIM and yTIM. Native EhTIM and yTIM were subjected to hydrostatic pressure jumps up to 350 MPa. A gradual red shift of up to 4 nm (EhTIM) and 2 nm (yTIM) in the SCM was observed (Figures 4 and 5, respectively), indicating that the dissociation and/or unfolding transition detected is not complete within this pressure range. A series of refolded EhTIM (0.7−1.2 M GdnHCl) and yTIM samples (0.7−1.1 M GdnHCl) were subjected to a high-pressure cycle. According to

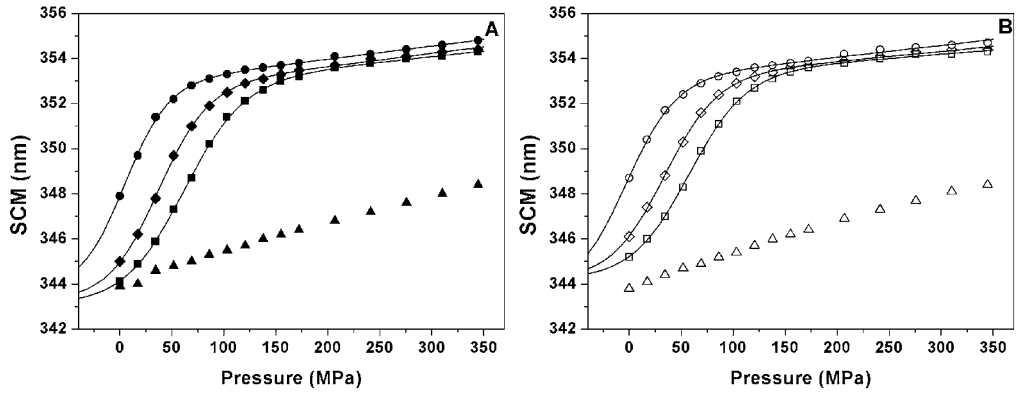

FIGURE 4: Effect of pressure on EhTIM. Native EhTIM (▲ and △) and EhTIM samples refolded in 0.7 (■ and □), 0.9 (◆ and ◇), or 1.1 M GdnHCl (● and ○) were incubated for 24 h. Samples were then subjected to pressurization (A) and depressurization (B). SCM was calculated from emission spectra taken 30 min after each pressure jump. Solid lines are fits to eq 4; fitting parameters are listed in Table 3.

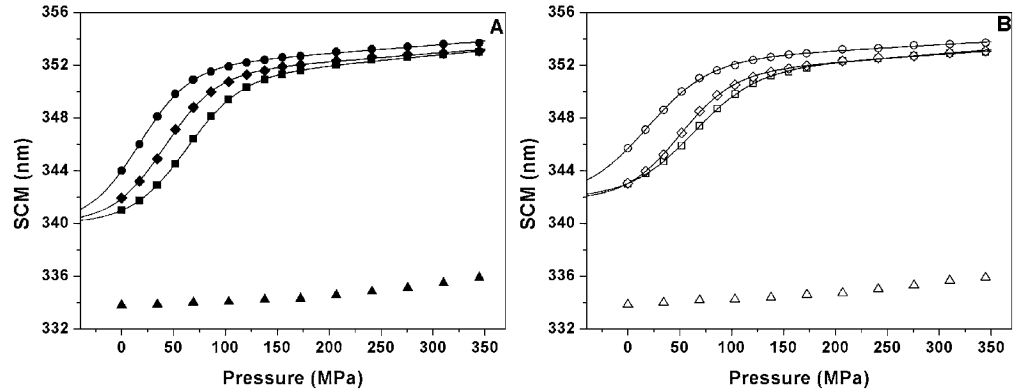

FIGURE 5: Effect of pressure on yTIM. Native yTIM (▲ and △) and yTIM samples refolded in 0.7 (■ and □), 0.9 (◆ and ◇), or 1.1 M GdnHCl (● and ○) were incubated for 24 h. Samples were then subjected to pressurization (A) and depressurization (B). SCM was calculated from emission spectra taken 30 min after each pressure jump. Solid lines are fits to eq 4; fitting parameters are listed in Table 4.

Table 3: Thermodynamic Properties of EhTIM Unfolding and Refolding by Pressure[a]

	pressurization			depressurization		
[GdnHCl]	ΔG_{Unf} (kJ/mol)	ΔV_{Unf} (mL/mol)	$P_{1/2}$ (MPa)	ΔG_{Unf} (kJ/mol)	ΔV_{Unf} (mL/mol)	$P_{1/2}$ (MPa)
0.7	5.2 ± 0.2	−86 ± 2	60	4.9 ± 0.2	−89 ± 2	55
0.8	4.4 ± 0.2	−96 ± 2	45	4.5 ± 0.3	−98 ± 4	46
0.9	3.7 ± 0.3	−104 ± 5	35	3.1 ± 0.3	−97 ± 4	32
1	4.2 ± 0.6	−117 ± 9	36	2.5 ± 0.3	−100 ± 4	26
1.1	2.4 ± 0.8	−111 ± 1	21	1.3 ± 0.1	−110 ± 4	12
1.2	0.4 ± 0.6	−119 ± 9	3.6	−0.4 ± 0.1	−105 ± 4	−3.9

[a] Figure 4 data were fitted to eq 4 using SCM_M as a fitting parameter. For pressurization data, the average SCM_M was 343.6 ± 0.55 nm. For depressurization data, the average SCM_M was 343.3 ± 1.48 nm.

Figures 2 and 3, the highest fraction of monomeric intermediate for EhTIM should be present in this range of denaturant concentration. From the data of Nájera et al. (*48*), the mole fraction of the yTIM monomeric intermediate varies from 0.92 to 0.77 over this range of denaturant concentrations. Pressure induced a single cooperative transition in all samples (representative experiments are shown in Figures 4 and 5).

The final observed SCM values were comparable to those obtained for both TIMs at high GdnHCl concentrations and atmospheric pressure. A slight linear change in the SCM was observed at high pressures, and this effect has been previously documented and is attributed to changes in the properties of water molecules solvating exposed aromatic residues (*72*). Small hysteresis was observed between pressurization and depressurization data [maximum $\Delta P_{1/2}$ = 10.8 MPa for EhTIM; maximum $\Delta P_{1/2}$ = 5.9 MPa for yTIM (Tables 3 and 4)]. With regard to reversibility, the difference between the SCM before and after the pressure cycle was close to 1 nm for EhTIM and 2 nm for yTIM. This indicates that the unfolding−refolding cycles induced by pressure were essentially reversible and at equilibrium. The proposed unimolecular nature of the pressure-induced transition was tested by assessing the effect of protein concentration on $P_{1/2}$. In this regard, recently, Ferreira and co-workers reported that in the presence of 0.4 M GdnHCl, a 10-fold increase in protein concentration produced a $\Delta P_{1/2}$ of 40.6 MPa in the pressure-induced dissociation of rTIM (*73*). In this work, in the presence of 1.2 M GdnHCl, a 4-fold increase in EhTIM concentration had no effect on the $P_{1/2}$ of the transition (data not shown). Likewise, in the presence of 0.7 M GdnHCl, a 13-fold increase in yTIM concentration produced a change

Table 4: Thermodynamic Properties of yTIM Unfolding and Refolding by Pressure[a]

	pressurization			depressurization		
[GdnHCl]	ΔG_{Unf} (kJ/mol)	ΔV_{Unf} (mL/mol)	$P_{1/2}$ (MPa)	ΔG_{Unf} (kJ/mol)	ΔV_{Unf} (mL/mol)	$P_{1/2}$ (MPa)
0.7	5.2 ± 0.2	-86 ± 2	60	4.9 ± 0.2	-89 ± 2	55
0.8	4.4 ± 0.2	-96 ± 2	45	4.5 ± 0.3	-98 ± 4	46
0.9	3.7 ± 0.3	-104 ± 5	35	3.1 ± 0.3	-97 ± 4	32
1	4.2 ± 0.6	-117 ± 9	36	2.5 ± 0.3	-100 ± 4	26
1.1	2.4 ± 0.8	-111 ± 1	21	1.3 ± 0.1	-110 ± 4	12
1.2	0.4 ± 0.6	-119 ± 9	3.6	-0.4 ± 0.1	-105 ± 4	-3.9

[a] The data of Figure 5 were fitted to eq 4 using SCM_M as a fitting parameter. For pressurization data, the average SCM_M was 339.6 ± 0.86 nm. For depressurization data, the average SCM_M was 341.5 ± 1.04 nm.

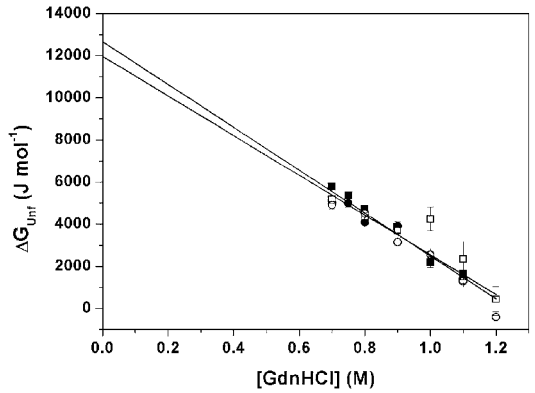

FIGURE 6: Free energy changes as a function of GdnHCl concentration. ΔG_{Unf} values from pressurization (squares) and depressurization (circles) were simultaneously fitted to eq 7 for yTIM (■ and ●) or EhTIM (□ and ○). Parameters are listed in Table 5.

of only 3.6 MPa in $P_{1/2}$ (data not shown), thus supporting the proposed monomeric nature of the folding intermediates. To obtain the thermodynamic properties of these processes, data from Figures 4 and 5 were analyzed with a two-state unfolding model (Tables 3 and 4). It was found that ΔG_{Unf} and $P_{1/2}$ decrease with an increasing concentration of denaturant, whereas ΔV_{Unf} becomes more negative in the presence of GdnHCl (Tables 3 and 4). In spite of the small hysteresis observed between pressurization and depressurization data sets, similar ΔG_{Unf}, ΔV_{Unf}, and $P_{1/2}$ values resulted from the fit of both data sets.

Comparison of the Thermodynamic Parameters Calculated for the Monomeric Intermediates in the Absence of Denaturant. To obtain the thermodynamic parameters for monomer unfolding in the absence of GdnHCl, ΔG_{Unf}, ΔV_{Unf}, and $P_{1/2}$ were linearly fitted against denaturant concentration using eq 7.

In accordance with atmospheric pressure unfolding studies (*6*), it was found that ΔG_{Unf} was correctly described as a linear function of GdnHCl concentration [$|r| > 0.824$ (Table 5)]. The ΔG_{UnfH_2O} value obtained for the simultaneous fit of pressurization and depressurization data for EhTIM [12.0 ± 1.2 kJ/mol (Table 5 and Figure 6)] is somewhat smaller than the ones obtained from the two-state global fit of spectroscopic data obtained in the presence of GdnHCl at atmospheric pressure [$\Delta G_{H_2O} = 16.2 \pm 1.1$ kJ/mol (Table 2)]. The ΔG_{UnfH_2O} value obtained for yTIM [12.7 ± 0.6 kJ/mol (Table 5)] is also lower than the ΔG_{UnfH_2O} previously reported (15.9−16.6 kJ/mol) from refolding experiments in GdnHCl followed from a global fit of catalytic activity, fluorescence SCM, CD, and R_s to a three-state model (*48*). The m_G value obtained for yTIM from pressure-data [-10.2 ± 0.68 kJ mol^{-1} M^{-1} (Table 4)] is close to the m_G value obtained from experiments carried out at atmospheric pressure [−12.2 to −12.4 kJ mol^{-1} M^{-1} (H. Nájera et al., manuscript submitted for publication)]. The m_G value obtained for EhTIM from pressure data [-9.4 ± 1.2 kJ mol^{-1} M^{-1} (Table 5)] is comparable to the m_G value obtained from experiments carried out at atmospheric pressure [-13.2 ± 0.85 kJ mol^{-1} M^{-1} (Table 2)]. The small differences between the ΔG_{UnfH_2O} and m_G values derived from high-pressure data and those obtained at atmospheric pressure suggest that the unfolded states induced by GdnHCl at atmospheric pressure and those observed by the combination of GdnHCl and high pressure may not be equivalent. Nonetheless, the similar stability calculated for the monomeric intermediates of EhTIM and yTIM indicates that the insertions observed in the loops connecting the α helices and β strands of the EhTIM barrel induce no significant stabilization of the barrel. The closeness in the ΔG_{UnfH_2O} values obtained in this work for EhTIM and yTIM contrasts with the high variation reported in the literature. For example, rabbit TIM $\Delta G_{UnfH_2O} = 5.0$ kJ/mol (*55*) on the other extreme, and $\Delta G_{UnfH_2O} =$ 10.5−16.3 kJ/mol for monomeric human TIM mutants (*54*, *74*). A comparison of these values with those reported for the dissociation step (67.6−83.3 kJ/mol) (*48*) confirms that most of the stability of TIM relies on dimerization.

Reports on the effect of denaturants on $P_{1/2}$ are scarce. The $P_{1/2}$ of staphylococcal nuclease has been reported to decrease in the presence of urea and $CaCl_2$ (*75*). The $P_{1/2}$ of Ure2 was also found to decrease with increasing concentrations of GdnHCl (*22*). $P_{1/2}$ values exhibited a decrease with increasing denaturant concentrations (Figure 7). This behavior may be related to the increasing destabilization effect of GdnHCl on the native state. These data are very well described ($R > 0.941$) when fitted to a linear model (eq 7). To the best of our knowledge, the linear dependence of $P_{1/2}$ with GdnHCl concentration has not been previously proposed.

The simultaneous fit of pressurization and depressurization data gives similar $P_{1/2H_2O}$ values for EhTIM and yTIM [133 ± 8 and 146 ± 6 MPa, respectively (Table 5 and Figure 7)]. This indicates that in the absence of denaturants and intermolecular contacts, both monomeric intermediates would unfold within the pressure range used in our experiments. Since no complete pressure unfolding of native TIM was observed, we propose that dimerization prevents the pressure unfolding of the monomer. In this respect, given the $\Delta G_{DissocH_2O}$ values reported for yTIM (∼75.0 kJ/mol) and assuming an average ΔV_{Dissoc} of ∼130 mL/mol (*14*, *76*, *77*), a $P_{1/2Dissoc}$ of ∼580 MPa is calculated. This explains why we were not able to detect the full pressure-induced dis-

Table 5: Thermodynamic Properties of yTIM and EhTIM Pressure-Induced Unfolding and Refolding in the Absence of GdnHCl[a]

	ΔG_{UnfH_2O}[a] (kJ/mol)	m_G[a] (kJ mol^{-1} M^{-1})	R	ΔV_{UnfH_2O}[b] (mL/mol)	ΔV_{UnfH_2O}[c] (mL/mol)	m_V[c] (mL mol^{-1} M^{-1})	R	$P_{1/2H_2O}$[d] (MPa)	m_P[d] (MPa M^{-1})	R
EhTIM press.	11.3 ± 1.9	−8.3 ± 1.9	−0.824	−106 ± 13	−46 ± 12	−63.1 ± 12.2	−0.870	129 ± 12	−101 ± 13	−0.941
EhTIM depress.	12.6 ± 1.0	−10.5 ± 0.9	−0.967	−100 ± 7	−68 ± 9	−34.0 ± 9.4	−0.766	138 ± 6	−116 ± 6	−0.989
EhTIM both sets	12.0 ± 1.2	−9.4 ± 1.2	−0.858	−103 ± 10	−57 ± 10	−48.5 ± 9.8	−0.710	133 ± 8	−108 ± 9	−0.940
yTIM press.	13.4 ± 0.6	−10.9 ± 0.7	−0.985	−98 ± 6	−69 ± 10	−33.1 ± 10.8	−0.700	150 ± 9	−125 ± 10	−0.975
yTIM depress.	11.9 ± 0.9	−9.5 ± 1.0	−0.958	−86 ± 3	−83 ± 9	−3.8 ± 9.7	−0.036	142 ± 9	−114 ± 10	−0.970
yTIM both sets	12.7 ± 0.6	−10.2 ± 0.7	−0.957	−92 ± 8	−76 ± 14	−18.4 ± 15.9	−0.118	146 ± 6	−119 ± 7	−0.970

[a] ΔG_{UnfH_2O} and m_G were calculated with data from Figure 6 fitted to eq 7. [b] ΔV_{UnfH_2O} was calculated assuming ΔV_{Unf} is independent of denaturant concentration. [c] ΔV_{UnfH_2O} and m_V were calculated with data from Figure 7 fitted to eq 7. [d] $P_{1/2H_2O}$ and m_P were calculated with data from Figure 8 fitted to eq 7.

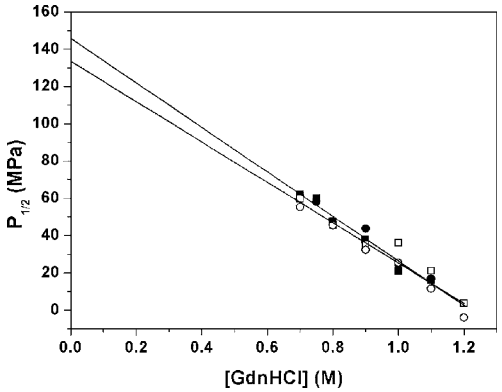

FIGURE 7: Dependence of $P_{1/2}$ on GdnHCl concentration. $P_{1/2}$ values from pressurization (squares) and depressurization (circles) were simultaneously fitted to eq 7 for yTIM (■ and ●) or EhTIM (□ and ○). Parameters are listed in Table 5.

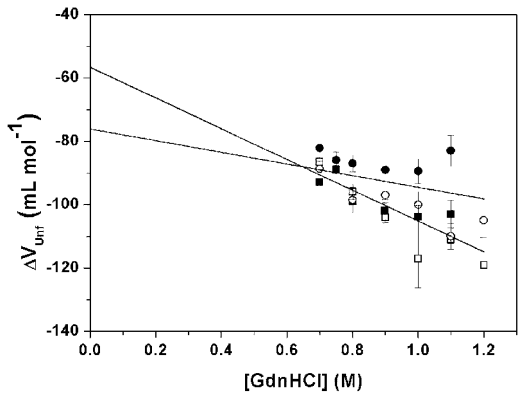

FIGURE 8: Volume changes as a function of GdnHCl concentration. ΔV_{Unf} values from pressurization (squares) and depressurization (circles) were simultaneously fitted to eq 7 for yTIM (■ and ●) or EhTIM (□ and ○). Parameters are listed in Table 5.

sociation of yTIM in the absence of denaturants. The unfolding of rTIM by hydrostatic pressure in the absence of denaturants has been studied by Rietveld and Ferreira; these authors observed a large hysteresis (∼150 MPa) between pressurization and depressurization data (*61*). From FRET measurements, these authors concluded that dissociation and unfolding took place concomitantly. This finding is in agreement with our data, since in the absence of denaturants we predict that monomer unfolding would take place at lower pressures than dissociation. The full profile of dissociation and unfolding could be followed by other high-pressure methodologies (*35*, *78*, *79*).

Although the ΔG_{Unf} and $P_{1/2}$ versus GdnHCl concentration data presented in Figures 6 and 7 show a clear linear tendency [$R > 0.824$ (Table 5)], ΔV_{Unf} values are somewhat scattered, particularly those obtained for yTIM depressurization [Figure 8 (●)]. ΔV_{UnfH_2O} was therefore calculated in two ways. (i) Assuming no dependence of ΔV_{Unf} on GdnHCl concentration, the mean ΔV_{UnfH_2O} values obtained for pressurization and depressurization data are -103 ± 10 and -92 ± 8 mL/mol for EhTIM and yTIM, respectively (see Table 5). (ii) On the other hand, when the linear model was applied (eq 7), the ΔV_{UnfH_2O} values obtained are -57 ± 10 mL/mol for EhTIM and -76 ± 14 mL/mol for yTIM (Table 5). In both approaches, the ΔV_{UnfH_2O} values obtained for EhTIM and yTIM are the same within experimental error. The ΔV_{UnfH_2O} values reported for the unfolding of monomeric proteins of comparable size (−90 to −120 mL/mol) (*77*) are similar to the ΔV_{UnfH_2O} values calculated for TIM assuming no dependence on GdnHCl concentration (−92 to −103 mL/mol) and more negative than those calculated using the linear model approach (−57 to −76 mL/mol).

It should be noted that besides the scattering observed in Figure 8 data, all data sets, except those from yTIM depressurization, show a considerable negative slope. For instance, $|\Delta V_{Unf}|$ increases in the presence of GdnHCl. The magnitude and particularly the physical basis of volume changes in protein folding remain controversial (*12*, *77*). In the case of staphylococcal nuclease, ΔV_{Unf} can be independent, decreasing or increasing depending on the chosen cosolvent (*75*). ΔV_{Unf} values reported in the literature have usually been found to be independent of GdnHCl concentration (*22*, *26*, *32*, *79*). Exceptions to this behavior have been documented for hen egg white lisozyme at low temperatures, where $|\Delta V_{Unf}|$ decreases with denaturant concentration (*34*) and human apolipoprotein A-I, where $|\Delta V_{Unf}|$ increases in the presence of GdnHCl (*27*). The change in ΔV_{Unf} with denaturant concentration suggests that the intrinsic volumes and/or the solvation properties of the monomeric intermediate or the unfolded monomers are modified by GdnHCl. Two main effects should be considered. First, since unfolded states present more exposed area than native states and GdnHCl binds to the protein surface, the level of preferential binding should increase with denaturant concentration (*80*). This would decrease the degree of hydration; concomitantly, $|\Delta V_{Unf}|$ should decrease when GdnHCl is present. The opposite was observed; therefore, a possible source for an increase in $|\Delta V_{Unf}|$ is a more unfolded state in the presence of denaturant. A similar explanation was proposed for the increase in $|\Delta V_{Unf}|$ with $CaCl_2$ concentration reported in the pressure-induced unfolding of staphylococcal nuclease (*75*). Since both Gdn^+ and Ca^{2+} exhibit similar ionic effects according to Hofmeister series, it is possible that the effect of these denaturants on the unfolded state is related to their

water structure breaking properties (*81*, *82*). The results presented in this work indicate that valuable thermodynamic information regarding the properties of folding intermediates can be obtained from the combined use of pressure and chemical denaturants (*83*).

ACKNOWLEDGMENT

We thank Prof. Mario Calcagno for helpful suggestions. We thank Prof. J. Knowles for the gift of the yTIM gene.

REFERENCES

1. Mei, G., Di Venere, A., Rosato, N., and Finazzi-Agro, A. (2005) The importance of being dimeric, *FEBS J. 272*, 16−27.
2. Jaenicke, R., and Lilie, H. (2000) Folding and association of oligomeric and multimeric proteins, *Adv. Protein Chem. 53*, 329−401.
3. Jaenicke, R., and Rudolph, R. (1986) Refolding and association of oligomeric proteins, *Methods Enzymol. 131*, 218−250.
4. Jaenicke, R. (1988) Stability and self-organization of proteins, *Naturwissenschaften 75*, 604−610.
5. Neet, K. E., and Timm, D. E. (1994) Conformational stability of dimeric proteins: Quantitative studies by equilibrium denaturation, *Protein Sci. 3*, 2167−2174.
6. Pace, C. N. (1986) Determination and analysis of urea and guanidine hydrochloride denaturation curves, *Methods Enzymol. 131*, 266−280.
7. Pace, C. N. (1990) Measuring and increasing protein stability, *Trends Biotechnol. 8*, 93−98.
8. Pace, C. N. (1990) Conformational stability of globular proteins, *Trends Biochem. Sci. 15*, 14−17.
9. Pace, C. N., Laurents, D. V., and Thomson, J. A. (1990) pH dependence of the urea and guanidine hydrochloride denaturation of ribonuclease A and ribonuclease T1, *Biochemistry 29*, 2564−2572.
10. Silva, J. L., and Weber, G. (1993) Pressure stability of proteins, *Annu. Rev. Phys. Chem. 44*, 89−113.
11. Gross, M., and Jaenicke, R. (1994) Proteins under pressure. The influence of high hydrostatic pressure on structure, function and assembly of proteins and protein complexes, *Eur. J. Biochem. 221*, 617−630.
12. Royer, C. A. (2005) Insights into the role of hydration in protein structure and stability obtained through hydrostatic pressure studies, *Braz. J. Med. Biol. Res. 38*, 1167−1173.
13. Silva, J. L., Foguel, D., and Royer, C. A. (2001) Pressure provides new insights into protein folding, dynamics and structure, *Trends Biochem. Sci. 26*, 612−618.
14. Ruan, K., and Weber, G. (1988) Dissociation of yeast hexokinase by hydrostatic pressure, *Biochemistry 27*, 3295−3301.
15. Paladini, A. A., Jr., and Weber, G. (1981) Pressure-induced reversible dissociation of enolase, *Biochemistry 20*, 2587−2593.
16. Erijman, L., Lorimer, G. H., and Weber, G. (1993) Reversible dissociation and conformational stability of dimeric ribulose bisphosphate carboxylase, *Biochemistry 32*, 5187−5195.
17. Brandts, J. F., Oliveira, R. J., and Westort, C. (1970) Thermodynamics of protein denaturation. Effect of pressure on the denaturation of ribonuclease A, *Biochemistry 9*, 1038−1047.
18. Vidugiris, G. J., Truckses, D. M., Markley, J. L., and Royer, C. A. (1996) High-pressure denaturation of staphylococcal nuclease proline-to-glycine substitution mutants, *Biochemistry 35*, 3857−3864.
19. Vidugiris, G. J., and Royer, C. A. (1998) Determination of the volume changes for pressure-induced transitions of apomyoglobin between the native, molten globule, and unfolded states, *Biophys. J. 75*, 463−470.
20. Panick, G., Malessa, R., Winter, R., Rapp, G., Frye, K. J., and Royer, C. A. (1998) Structural characterization of the pressure-denatured state and unfolding/refolding kinetics of staphylococcal nuclease by synchrotron small-angle X-ray scattering and Fourier-transform infrared spectroscopy, *J. Mol. Biol. 275*, 389−402.
21. Panick, G., Vidugiris, G. J., Malessa, R., Rapp, G., Winter, R., and Royer, C. A. (1999) Exploring the temperature-pressure phase diagram of staphylococcal nuclease, *Biochemistry 38*, 4157−4164.
22. Zhou, J. M., Zhu, L., Balny, C., and Perrett, S. (2001) Pressure denaturation of the yeast prion protein Ure2, *Biochem. Biophys. Res. Commun. 287*, 147−152.
23. Mohana-Borges, R., Silva, J. L., Ruiz-Sanz, J., and de Prat-Gay, G. (1999) Folding of a pressure-denatured model protein, *Proc. Natl. Acad. Sci. U.S.A. 96*, 7888−7893.
24. Chapeaurouge, A., Johansson, J. S., and Ferreira, S. T. (2001) Folding intermediates of a model three-helix bundle protein. Pressure and cold denaturation studies, *J. Biol. Chem. 276*, 14861−14866.
25. Bismuto, E., Sirangelo, I., Irace, G., and Gratton, E. (1996) Pressure-induced perturbation of apomyoglobin structure: Fluorescence studies on native and acidic compact forms, *Biochemistry 35*, 1173−1178.
26. Kobashigawa, Y., Sakurai, M., and Nitta, K. (1999) Effect of hydrostatic pressure on unfolding of α-lactalbumin: Volumetric equivalence of the molten globule and unfolded state, *Protein Sci. 8*, 2765−2772.
27. Mantulin, W. W., and Pownall, H. J. (1985) Reversible folding reactions of human apolipoprotein A-I: Pressure and guanidinium chloride effects, *Biochim. Biophys. Acta 836*, 215−221.
28. Foguel, D., Robinson, C. R., de Sousa, P. C., Jr., Silva, J. L., and Robinson, A. S. (1999) Hydrostatic pressure rescues native protein from aggregates, *Biotechnol. Bioeng. 63*, 552−558.
29. Ferreira, S. T., Chapeaurouge, A., and De Felice, F. G. (2005) Stabilization of partially folded states in protein folding/misfolding transitions by hydrostatic pressure, *Braz. J. Med. Biol. Res. 38*, 1215−1222.
30. Ferreira, S. T., De Felice, F. G., and Chapeaurouge, A. (2006) Metastable, partially folded states in the productive folding and in the misfolding and amyloid aggregation of proteins, *Cell Biochem. Biophys. 44*, 539−548.
31. Ferrao-Gonzales, A. D., Souto, S. O., Silva, J. L., and Foguel, D. (2000) The preaggregated state of an amyloidogenic protein: Hydrostatic pressure converts native transthyretin into the amyloidogenic state, *Proc. Natl. Acad. Sci. U.S.A. 97*, 6445−6450.
32. Sasahara, K., and Nitta, K. (1999) Pressure-induced unfolding of lysozyme in aqueous guanidinium chloride solution, *Protein Sci. 8*, 1469−1474.
33. Sasahara, K., Sakurai, M., and Nitta, K. (1999) The volume and compressibility changes of lysozyme associated with guanidinium chloride and pressure-assisted unfolding, *J. Mol. Biol. 291*, 693−701.
34. Sasahara, K., Sakurai, M., and Nitta, K. (2001) Pressure effect on denaturant-induced unfolding of hen egg white lysozyme, *Proteins 44*, 180−187.
35. Zhou, J. M., Zhu, L., and Balny, C. (2000) Inactivation of creatine kinase by high pressure may precede dimer dissociation, *Eur. J. Biochem. 267*, 1247−1253.
36. Knowles, J. R., and Albery, J. W. (1977) Perfection in enzyme catalysis: The energetics of triosephosphate isomerase, *Acc. Chem. Res. 10*, 105−111.
37. Knowles, J. R. (1991) Enzyme catalysis: Not different, just better, *Nature 350*, 121−124.
38. Lolis, E., Alber, T., Davenport, R. C., Rose, D., Hartman, F. C., and Petsko, G. A. (1990) Structure of yeast triosephosphate isomerase at 1.9-Å resolution, *Biochemistry 29*, 6609−6618.
39. Rozovsky, S., Jogl, G., Tong, L., and McDermott, A. E. (2001) Solution-state NMR investigations of triosephosphate isomerase active site loop motion: Ligand release in relation to active site loop dynamics, *J. Mol. Biol. 310*, 271−280.
40. Jogl, G., Rozovsky, S., McDermott, A. E., and Tong, L. (2003) Optimal alignment for enzymatic proton transfer: Structure of the Michaelis complex of triosephosphate isomerase at 1.2-Å resolution, *Proc. Natl. Acad. Sci. U.S.A. 100*, 50−55.
41. Xiang, J., Jung, J. Y., and Sampson, N. S. (2004) Entropy effects on protein hinges: The reaction catalyzed by triosephosphate isomerase, *Biochemistry 43*, 11436−11445.
42. Blacklow, S. C., Raines, R. T., Lim, W. A., Zamore, P. D., and Knowles, J. R. (1988) Triosephosphate isomerase catalysis is diffusion controlled. Appendix: Analysis of triose phosphate equilibria in aqueous solution by ^{31}P NMR, *Biochemistry 27*, 1158−1167.
43. Waley, S. G. (1973) Refolding of triose phosphate isomerase, *Biochem. J. 135*, 165−172.
44. Zabori, S., Rudolph, R., and Jaenicke, R. (1980) Folding and association of triose phosphate isomerase from rabbit muscle, *Z. Naturforsch. C35*, 999−1004.
45. Garza-Ramos, G., Tuena de Gómez-Puyou, M., Gómez-Puyou, A., and Gracy, R. W. (1992) Dimerization and reactivation of triosephosphate isomerase in reverse micelles, *Eur. J. Biochem. 208*, 389−395.

46. Fernández-Velasco, D. A., Sepúlveda-Becerra, M., Galina, A., Darszon, A., Tuena de Gómez-Puyou, M., and Gómez-Puyou, A. (1995) Water requirements in monomer folding and dimerization of triosephosphate isomerase in reverse micelles. Intrinsic fluorescence of conformers related to reactivation, *Biochemistry 34*, 361−369.
47. Chánez-Cárdenas, M. E., Fernández-Velasco, D. A., Vázquez-Contreras, E., Coria, R., Saab-Rincon, G., and Pérez-Montfort, R. (2002) Unfolding of triosephosphate isomerase from *Trypanosoma brucei*: Identification of intermediates and insight into the denaturation pathway using tryptophan mutants, *Arch. Biochem. Biophys. 399*, 117−129.
48. Nájera, H., Costas, M., and Fernández-Velasco, D. A. (2003) Thermodynamic characterization of yeast triosephosphate isomerase refolding: Insights into the interplay between function and stability as reasons for the oligomeric nature of the enzyme, *Biochem. J. 370*, 785−792.
49. Chánez-Cárdenas, M. E., Pérez-Hernandez, G., Sanchez-Rebollar, B. G., Costas, M., and Vázquez-Contreras, E. (2005) Reversible equilibrium unfolding of triosephosphate isomerase from *Trypanosoma cruzi* in guanidinium hydrochloride involves stable dimeric and monomeric intermediates, *Biochemistry 44*, 10883−10892.
50. Rodriguez-Romero, A., Hernandez-Santoyo, A., del Pozo Yauner, L., Kornhauser, A., and Fernández-Velasco, D. A. (2002) Structure and inactivation of triosephosphate isomerase from *Entamoeba histolytica*, *J. Mol. Biol. 322*, 669−675.
51. Borchert, T. V., Abagyan, R., Jaenicke, R., and Wierenga, R. K. (1994) Design, creation, and characterization of a stable, monomeric triosephosphate isomerase, *Proc. Natl. Acad. Sci. U.S.A. 91*, 1515−1518.
52. Schliebs, W., Thanki, N., Jaenicke, R., and Wierenga, R. K. (1997) A double mutation at the tip of the dimer interface loop of triosephosphate isomerase generates active monomers with reduced stability, *Biochemistry 36*, 9655−9662.
53. Saab-Rincón, G., Juárez, V. R., Osuna, J., Sánchez, F., and Soberón, X. (2001) Different strategies to recover the activity of monomeric triosephosphate isomerase by directed evolution, *Protein Eng. 14*, 149−155.
54. Mainfroid, V., Mande, S. C., Hol, W. G., Martial, J. A., and Goraj, K. (1996) Stabilization of human triosephosphate isomerase by improvement of the stability of individual α-helices in dimeric as well as monomeric forms of the protein, *Biochemistry 35*, 4110−4117.
55. Rietveld, A. W., and Ferreira, S. T. (1998) Kinetics and energetics of subunit dissociation/unfolding of TIM: The importance of oligomerization for conformational persistence and chemical stability of proteins, *Biochemistry 37*, 933−937.
56. Pan, H., Raza, A. S., and Smith, D. L. (2004) Equilibrium and kinetic folding of rabbit muscle triosephosphate isomerase by hydrogen exchange mass spectrometry, *J. Mol. Biol. 336*, 1251−1263.
57. Gokhale, R. S., Ray, S. S., Balaram, H., and Balaram, P. (1999) Unfolding of *Plasmodium falciparum* triosephosphate isomerase in urea and guanidinium chloride: Evidence for a novel disulfide exchange reaction in a covalently cross-linked mutant, *Biochemistry 38*, 423−431.
58. Lambeir, A. M., Backmann, J., Ruiz-Sanz, J., Filimonov, V., Nielsen, J. E., Kursula, I., Norledge, B. V., and Wierenga, R. K. (2000) The ionization of a buried glutamic acid is thermodynamically linked to the stability of *Leishmania mexicana* triose phosphate isomerase, *Eur. J. Biochem. 267*, 2516−2524.
59. Zomosa-Signoret, V., Hernández-Alcántara, G., Reyes-Vivas, H., Martínez-Martínez, E., Garza-Ramos, G., Pérez-Montfort, R., Tuena De Gómez-Puyou, M., and Gómez-Puyou, A. (2003) Control of the reactivation kinetics of homodimeric triosephosphate isomerase from unfolded monomers, *Biochemistry 42*, 3311−3318.
60. Silverman, J. A., and Harbury, P. B. (2002) The equilibrium unfolding pathway of a $(\beta/\alpha)_8$ barrel, *J. Mol. Biol. 240*, 184−187.
61. Rietveld, A. W., and Ferreira, S. T. (1996) Deterministic pressure dissociation and unfolding of triose phosphate isomerase: Persistent heterogeneity of a protein dimer, *Biochemistry 35*, 7743−7751.
62. Moreau, V. H., Rietveld, A. W., and Ferreira, S. T. (2003) Persistent conformational heterogeneity of triosephosphate isomerase: Separation and characterization of conformational isomers in solution, *Biochemistry 42*, 14831−14837.
63. Morgan, C. J., Wilkins, D. K., Smith, L. J., Kawata, Y., and Dobson, C. M. (2000) A compact monomeric intermediate identified by NMR in the denaturation of dimeric triose phosphate isomerase, *J. Mol. Biol. 300*, 11−16.
64. Benítez-Cardoza, C. G., Rojo-Domínguez, A., and Hernández-Arana, A. (2001) Temperature-induced denaturation and renaturation of triosephosphate isomerase from *Saccharomyces cerevisiae*: Evidence of dimerization coupled to refolding of the thermally unfolded protein, *Biochemistry 40*, 9049−9058.
65. González-Mondragón, E., Zubillaga, R. A., Saavedra, E., Chánez-Cárdenas, M. E., Pérez-Montfort, R., and Hernández-Arana, A. (2004) Conserved cysteine 126 in triosephosphate isomerase is required not for enzymatic activity but for proper folding and stability, *Biochemistry 43*, 3255−3263.
66. Vázquez-Contreras, E., Zubillaga, R., Mendoza-Hernández, G., Costas, M., and Fernández-Velasco, D. A. (2000) Equilibrium unfolding of yeast triosephosphate isomerase: A monomeric intermediate in guanidine-HCl and two-state behaviour in urea, *Protein Pept. Lett. 7*, 57−64.
67. Landa, A., Rojo-Domínguez, A., Jiménez, L., and Fernández-Velasco, D. A. (1997) Sequencing, expression and properties of triosephosphate isomerase from *Entamoeba histolytica*, *Eur. J. Biochem. 247*, 348−355.
68. Lakowicz, J. R. (1999) *Principles of fluorescence spectroscopy*, 2nd ed., Kluwer Academic/Plenum, New York.
69. Ruan, K., Tian, S., Lange, R., and Balny, C. (2000) Pressure effects on tryptophan and its derivatives, *Biochem. Biophys. Res. Commun. 269*, 681−686.
70. Eftink, M. R., and Ghiron, C. A. (1976) Exposure of tryptophanyl residues in proteins. Quantitative determination by fluorescence quenching studies, *Biochemistry 15*, 672−680.
71. Hill, B. C., Horowitz, P. M., and Robinson, N. C. (1986) Detection, characterization, and quenching of the intrinsic fluorescence of bovine heart cytochrome c oxidase, *Biochemistry 25*, 2287−2292.
72. Chattopadhyay, A., Rawat, S. S., Kelkar, D. A., Ray, S., and Chakrabarti, A. (2003) Organization and dynamics of tryptophan residues in erythroid spectrin: Novel structural features of denatured spectrin revealed by the wavelength-selective fluorescence approach, *Protein Sci. 12*, 2389−2403.
73. Botelho, M. G., Rietveld, A. W. M., and Ferreira, S. T. (2006) Long-lived conformational isomerism of protein dimers: The role of the free-energy of subunit association, *Biophys. J. 91*, 2826−2832.
74. Mainfroid, V., Terpstra, P., Beauregard, M., Frere, J. M., Mande, S. C., Hol, W. G., Martial, J. A., and Goraj, K. (1996) Three hTIM mutants that provide new insights on why TIM is a dimer, *J. Mol. Biol. 257*, 441−456.
75. Herberhold, H., Royer, C. A., and Winter, R. (2004) Effects of chaotropic and kosmotropic cosolvents on the pressure-induced unfolding and denaturation of proteins: An FT-IR study on staphylococcal nuclease, *Biochemistry 43*, 3336−3345.
76. Erijman, L., and Weber, G. (1991) Oligomeric protein associations: Transition from stochastic to deterministic equilibrium, *Biochemistry 30*, 1595−1599.
77. Royer, C. A. (2002) Revisiting volume changes in pressure-induced protein unfolding, *Biochim. Biophys. Acta 1595*, 201−209.
78. Akasaka, K. (2003) Highly fluctuating protein structures revealed by variable-pressure nuclear magnetic resonance, *Biochemistry 42*, 10875−10885.
79. Pappenberger, G., Saudan, C., Becker, M., Merbach, A. E., and Kiefhaber, T. (2000) Denaturant-induced movement of the transition state of protein folding revealed by high-pressure stopped-flow measurements, *Proc. Natl. Acad. Sci. U.S.A. 97*, 17−22.
80. Timasheff, S. N., and Arakawa, T. (1989) Stabilization of protein structure by solvents, in *Protein Structure: A Practical Approach* (Creighton, T. E., Ed.) pp 331−335, IRL Press, Oxford, U.K.
81. Von Hippel, P. H., and Wong, K. W. (1965) On the Conformational Stability of Globular Proteins, *J. Biol. Chem. 240*, 3909−3923.
82. Batchelor, J. D., Olteanu, A., Tripathy, A., and Pielak, G. J. (2004) Impact of protein denaturants and stabilizers on water structure. *J. Am. Chem. Soc. 126*, 1958−1961.
83. Perrett, S., and Zhou, J. M. (2002) Expanding the pressure technique: Insights into protein folding from combined use of pressure and chemical denaturants, *Biochim. Biophys. Acta 1595*, 210−223.

BI061879J